Thermal convection with shear at high Rayleigh number

By ANDREW P. INGERSOLL

Pierce Hall, Harvard University

A fluid is contained between rigid horizontal planes which move relative to each other with constant horizontal velocity. A gravitationally unstable temperature difference is maintained at the boundaries, and the heat flux and momentum flux (stress) transmitted by the fluid are measured. The Nusselt number, Nu, and the dimensionless momentum flux, Mo, are obtained for small mean rates of shear. The Rayleigh number, R, and the Prandtl number, σ, are both large in these experiments. The data are consistent with the following relations:

$$Nu \propto Mo\sigma^{\frac{1}{2}} \propto R^{\frac{1}{3}}.$$

Kraichnan's mixing-length theory of turbulent thermal convection is extended to the present situation, and the above experimental dependence of Nu and Mo on R and σ is obtained. The agreement between mixing-length theory and experiment provides strong support for Kraichnan's concise treatment of turbulent convection. The importance of this result is that heat and momentum fluxes may be calculated in this way for a variety of flows in geophysics.

1. Introduction

In the atmosphere and the oceans, thermal convection usually occurs in the presence of a mean velocity. Nevertheless, it has been useful in the past to study convection with no mean flow in order to understand the phenomenon in its simplest form. In the present study, we consider convection between rigid horizontal boundaries which move relative to each other with constant velocity. In seeking to understand this relatively simple example of convection with shear, which can be studied theoretically and in the laboratory, we hope to gain greater insight into more complicated geophysical situations.

The mathematical model is a Boussinesq fluid contained between horizontal surfaces on which the temperature and velocity are constant. The lower boundary is maintained at a temperature ΔT above that of the upper boundary, and the two surfaces move horizontally relative to each other with velocity ΔU.

We have been able to approximate this situation in the laboratory with a liquid contained between horizontal metal disks, one of which rotates about a vertical axis. The radii of the disks were large compared with their separation, and for small enough rotation rates it was possible to neglect the effects of curvature and centrifugal acceleration. By measuring the net heat transport and the

14

torque on the non-rotating disk, we could calculate the vertical fluxes of heat and horizontal momentum as functions of the independent variables of the problem.

The above experimental design has several advantages. A major difficulty in studying shear flow in a straight channel is the spatial inhomogeneity introduced at the ends of the channel. In a circular geometry this difficulty cannot arise. In addition, this geometry enables one to compute shear stress by measuring torque, whereas stress measurements in a straight channel would be more difficult. On the other hand, in order to minimize the dynamical effects of the circular geometry, one is limited to small rotation rates, and therefore to small rates of shear. Thus it was not possible to model the shear-induced turbulence which occurs in the atmosphere near the ground. Rather, convective turbulence dominated the flow in this experiment, as in the atmosphere above the shear layer during unstable conditions.

A rather striking feature of the experimental data is that the mean fluxes become independent of the plate separation d, for d large. This also appears in the heat-flux measurements without shear of Malkus (1954a), Silveston (1958), and Globe & Dropkin (1959). Thus it is reasonable to analyse the flow near the boundaries using mixing-length theory, assuming that the external length scale d does not enter the problem. This is the basis of Kraichnan's (1962) mixing-length theory, which we have extended to turbulent thermal convection with a small superimposed shear. The observed dependence of the fluxes on the physical constants of the problem was obtained in this way. Specifically, this theory accurately predicts the dependence of the dimensionless momentum flux on the Prandtl number σ, and on the Rayleigh number R for σ and R large. It has been difficult, from previous experiments, to assess the effect of σ on the dimensionless heat flux. And so by measuring momentum flux, we now have a new and stronger test of Kraichnan's theory.

Our experiment thus adds new support to Kraichnan's concise treatment of turbulent thermal convection. It also represents a first step in treating problems of convection with shear. One hopes that the mixing-length approach will lead to the development of more rigorous solutions of both problems, and that this will lead to a better understanding of turbulent flows near solid boundaries.

2. Summary of theoretical predictions

2.1. *Definitions and formulae*

We assume that the fluid obeys the Boussinesq equations of motion (Chandrasekhar 1961, p. 18). Let $\mathbf{v} = (u, v, w)$ be the velocity at time t at a point (x, y, z) in the fluid, where z is the vertical co-ordinate. Let T be the temperature of the fluid at (x, y, z, t). The boundary conditions are

$$\begin{aligned} \mathbf{v} &= (0, 0, 0), & T &= 0 & \text{at} \quad z &= 0, \\ \mathbf{v} &= (\Delta U, 0, 0), & T &= -\Delta T & \text{at} \quad z &= d. \end{aligned} \right\} \tag{1}$$

We also assume that all properties have bounded variation horizontally. Then

taking the horizontal mean of the Boussinesq equations, one obtains the constants

$$H = -\kappa(d\bar{T}/dz) + \overline{wT}, \tag{2}$$

$$M = \nu(d\bar{u}/dz) - \overline{wu}, \tag{3}$$

where κ is the thermometric conductivity and ν the kinematic viscosity of the fluid. The horizontal average is denoted by a single bar.

The quantities H and M are proportional to the mean upward fluxes of heat and horizontal momentum, respectively, and must be independent of z and t in a statistically steady state. Here we shall be more interested in the dimensionless fluxes; these are the Nusselt number Nu, and the momentum number Mo, where

$$Nu = (Hd/\kappa\Delta T), \quad Mo = (Md/\nu\Delta U). \tag{4}$$

In addition, we define the Prandtl number σ, the Reynolds number Re, and the Rayleigh number R. These are

$$\sigma = \nu/\kappa, \tag{5}$$

$$Re = \Delta U d/\nu, \tag{6}$$

$$R = \alpha g \Delta T d^3/(\nu\kappa), \tag{7}$$

where α is the thermal coefficient of expansion of the fluid and g is the acceleration of gravity. From dimensional reasoning, these three quantities are sufficient to determine the complete statistical structure of the flow, provided it is independent of the initial conditions after long time intervals.

2.2. *Formulation of the problem*

In general, we wish to find Nu and Mo as functions of the three independent variables of the problem, σ, Re and R. Here we shall consider only the case $\Delta U \rightarrow 0$ in the boundary conditions (1). Then it is convenient to divide the field of velocity, temperature and pressure into a convective part and a shear part, corresponding to the first two terms of a power-series expansion in the velocity ΔU. The convective field is assumed to satisfy the equations of thermal convection between stationary horizontal surfaces; the mean shear does not enter, and so to zero order in ΔU we will have

$$Nu = f_1(R, \sigma), \tag{8}$$

independent of the Reynolds number, Re.

Similarly, all shear quantities will be proportional to ΔU, to lowest order. That is, we neglect advection by the shear field relative to advection by the convective field. The motion of the fluid is driven by buoyancy forces, and the momentum due to the mean shear is simply a passive quantity which is convected by this field of motion. Therefore M will be proportional to ΔU, to this order, and from (4) we will have

$$Mo = f_2(R, \sigma). \tag{9}$$

The fact that Nu and Mo do not depend on Re follows from our assumption that the mean shear is small. In the experiment described below, we shall determine the limits of this assumption empirically.

The functional relationship (8) has been measured experimentally for various R and σ. See Malkus (1954 a), Globe & Dropkin (1959) and Silveston (1958), for examples of measurements of heat flux between stationary horizontal surfaces. Asymptotically at large R, the data are consistent with the following functional form:

$$Nu = g_1(\sigma) R^{\frac{1}{3}}, \tag{10}$$

with perhaps $\pm$ 10% uncertainty in the power $\frac{1}{3}$. From (4), (7) and (10), the heat flux H must be independent of the plate separation d, for d large. This implies that the magnitude of H is determined by small-scale flow near the boundaries, the structure of which is independent of d. Assuming this hypothesis to hold for the momentum flux M as well, equation (9) becomes

$$Mo = g_2(\sigma) R^{\frac{1}{3}}. \tag{11}$$

The function $g_1(\sigma)$ has been discussed theoretically by Malkus (1954 b, 1960), Kraichnan (1962), Herring (1964) and others. One may also extend these approaches to the equations in the shear quantities, in order to compute $g_2(\sigma)$, or more generally, the function $f_2(R, \sigma)$. Below we shall describe an approach based on Kraichnan's mixing-length theory. A solution of the mean field equations, as described by Herring for the convective field, is being sought at present.

2.3. *Mixing-length solution*

Kraichnan (1962) has treated the thermal convection problem using mixing-length theory to predict the functional form of $g_1(\sigma)$, and has included an estimate of the numerical constants of proportionality which appear. One distinguishes several boundary layers characterizing the role of molecular dissipation in the heat and momentum equations separately. We shall consider only the case σ large ($\sigma > 0 \cdot 1$, according to Kraichnan), and shall exclude shear boundary-layer effects, which may appear at extremely high Rayleigh numbers, well beyond our experimental range.

Let z_κ and z_ν be the heights at which eddy-diffusion effects become equal to molecular-diffusion effects in the heat and momentum equations, respectively. Then we may separate the flow in the lower half space into three regions:

$$\text{I.} \ \ 0 < z < z_\kappa, \qquad \text{II.} \ \ z_\kappa < z < z_\nu, \qquad \text{III.} \ \ z_\nu < z < \tfrac{1}{2}d,$$

for R and σ large enough. If $z_\kappa \ll z_\nu \ll \tfrac{1}{2}d$, it is reasonable to assume that each region may be treated separately, and that at each level the scale of the motion depends only on the height, z. This approach is equivalent to looking for similarity solutions within each region, under the assumption that the vertical and horizontal scales are equal at each level.

From (2), and the definition of z_κ, the mean temperature gradient at $z = z_\kappa$ will be one-half its value at the boundary. Therefore most of the temperature drop from $\overline{T} = 0$ at the boundary to $\overline{T} = -\tfrac{1}{2}\Delta T$ in the interior will take place in region I. This means, approximately,

$$H = -\kappa \frac{d\overline{T}}{dz}\bigg|_{z=0} \sim \frac{\kappa \Delta T}{2z_\kappa},$$

or

$$Nu \sim d/(2z_\kappa). \tag{12}$$

Similarly, one might say
$$Mo \sim d/(2z_\nu),$$
(13)

an assumption which we shall discuss further below.

One may obtain similarity solutions in regions II and III, assuming that molecular diffusion is only important in the momentum equation in region II, and is totally negligible in region III. Thus, for region II, conservation of vertical momentum yields
$$\nu \frac{\pi^2}{z^2} \tilde{w} \sim \alpha g \vartheta,$$
(14)

where $\tilde{w}$ and ϑ are the r.m.s. vertical velocity and fluctuating temperature, respectively. Equation (14) requires that advection by the velocity of the mean shear be negligible relative to buoyant accelerations. Similarly, the mean heat equation yields for region II,
$$\tilde{w}\vartheta \sim H.$$
(15)

Then, to find z_κ and z_ν, one must assume that the local Peclet number and the local Reynolds number [no relation to Re in (6)] assume definite transitional values at $z = z_\kappa$ and $z = z_\nu$, respectively. Thus Kraichnan requires
$$\tilde{w}(z_\kappa) z_\kappa / \kappa = Pe_T \sim 3,$$
(16)

$$\tilde{w}(z_\nu) z_\nu / \nu = Re_T \sim 30.$$
(17)

To evaluate $\tilde{w}$ at $z = z_\kappa$ and $z = z_\nu$, one extrapolates the similarity relations (14) and (15) to these levels. Then when equations (12) to (17) are combined one obtains, for large σ,
$$Nu \sim (12\pi)^{-\frac{2}{3}} R^{\frac{1}{3}},$$
(18)

$$Mo \sim (10)^{-\frac{1}{2}} Nu \sigma^{-\frac{1}{2}}.$$
(19)

Thus mixing-length theory predicts a definite functional dependence of Nu and Mo on R and σ, for R and σ large. This result is presumably only valid for $z_\kappa \ll z_\nu \ll \frac{1}{2}d$, which implies $Nu \gg Mo \gg 1$. Equations (18) and (19) also require that the mean shear be infinitesimal, since we neglected advection by the shear field in the above derivation.

We have not discussed the numerical constants which appear in equations (12) to (19). These are Kraichnan's estimates, based on general fluid mechanical arguments. Strictly speaking, $Re_T \sim 30$ is an estimate of the transition Reynolds number for diffusion of eddy momentum. Equation (13) assumes that this transition value is the same for the diffusion of mean momentum as well. Since this is not necessarily true, the value of the numerical constant in (19) is not to be taken seriously. We are more interested in testing the dependence of Nu and Mo on R and σ.

2.4. *Comment*

The preceding analysis is deceptively simple, and one may easily lose sight of the physical assumptions involved. We separated the flow near the boundary into three regions, and treated each region without introducing any inherent length scales. If this analysis is correct, then at each level z near the boundary, the transfer of heat and momentum is governed only by processes occurring at that level, of scale z. This assumption of local equilibrium at each level is analogous to Kolmogoroff's assumption concerning the cascade of energy to smaller

scales in a field of homogeneous turbulence (see Batchelor 1953, ch. VI). In our analysis, however, the turbulent interior region is not considered because the mean fluxes, and hence the energy of the motion throughout the fluid, are determined in the boundary-layer regions. Thus the molecular coefficients ν and κ will affect the intensity of the flow at all levels.

Note also that equations (18) and (19) imply nothing about the eddy viscosity or eddy conductivity in the turbulent interior region. Again, this is because the fluxes are controlled by the boundary layers, where molecular viscosity and conductivity are important, and where the concept of an eddy viscosity is less useful. On the other hand, if we extend the mixing-length analysis to region III we obtain

$$(\overline{T} + \tfrac{1}{2}\Delta T) \propto (\overline{u} - \tfrac{1}{2}\Delta u) \propto z^{-\frac{1}{3}},$$

which was predicted by Priestley (1959) and by Monin & Obukhov (1953). The eddy viscosity ν_e will then be proportional to the eddy conductivity κ_e, and given by

$$\nu_e \sim \kappa_e \sim (\alpha g H)^{\frac{1}{3}} z^{\frac{4}{3}}.$$

In order to test these relations, however, one would have to measure the profiles $\overline{T}(z)$ and $\overline{u}(z)$, which was not done in the present experiment.

Finally, we shall show that behaviour of the form (19) is not consistent with a straightforward extension of Malkus's (1954b, 1956, 1960) optimum mean field approach to transport phenomena. Malkus computes the mean temperature profile $\overline{T}(z)$ for which Nu is a maximum, subject to certain conditions. First, he requires that the mean temperature be expressible in terms of the lowest n_0 members of a set of orthogonal functions which satisfy the proper boundary conditions. The quantity n_0 is determined by requiring that disturbances of scale d/n_0 be marginally stable on the mean temperature field. Malkus's second condition is that the mean temperature gradient be negative or zero at all levels. The optimum Nu then depends only on n_0, which in turn depends only on R. The resulting curve $Nu(R)$ is quantitatively consistent with experiment for fluids of the Prandtl number greater than one.

Thus it is reasonable to compute the maximum value of Mo for convection with shear. For small rates of shear, the minimum scale should be unchanged, and so one expresses $\overline{u}(z)$ in terms of a series of orthogonal functions, truncated at order n_0. The other constraint will be a condition on the sign of one of the derivatives of $\overline{u}(z)$. Again, Mo will depend only on $n_0(R)$, and therefore cannot depend on the Prandtl number. This does not agree with (19), which we derived from mixing-length theory. On the other hand, one might argue that the optimum mean-field criterion should not apply to a passive quantity which has a negligible effect on the energy balance. Certainly Malkus's theory, as formulated above, cannot account for a dependence of Nu and Mo on the Prandtl number.

3. Experimental apparatus and procedures

3.1. *Principle of operation*

A liquid is contained in a shallow annular basin, defined by an inner and outer radius, and a flat, horizontal bottom. The upper surface of the liquid makes contact with a flat annular disk, which rotates at constant angular velocity

about the vertical axis of symmetry. The lower member does not rotate, and the vertical separation of the two horizontal surfaces is small compared to the other dimensions of the system. Then for small angular velocities, the flow in a short segment of the annulus will approximate straight rectilinear flow.

It was possible to measure the stress, or momentum flux between the surfaces by measuring the torque on the lower, stationary member due to the rotation of the upper member. This was done by supporting the lower member, which contains the fluid, on an air bearing, and by attaching a quartz fibre to it. One then obtains a measure of the momentum flux by noting the twist on the fibre necessary to balance the torque transmitted by the fluid. Of course, the mean velocity will vary linearly with distance from the axis, but for small enough rates of shear, the stress will also vary linearly with this distance. Then the stress at any radius may be easily computed from the total torque.

These rather delicate torque measurements demand that all other torques on the lower, floating member be strictly constant. We therefore chose to do a thermal decay-type experiment, in the manner used successfully by Malkus (1954a). Thus it was possible to heat the lower member and cool the upper member at the start of a run, and then to disconnect the heating apparatus before making torque measurements. The system decayed towards a steady isothermal state, but this approach was slow enough for a quasi-steady approximation to be made.

The average vertical heat flux was measured by noting the temperature drop across a pair of aluminium-formica-aluminium sandwiches in series with the upward flow of heat. This method was used both by Malkus (1954a), and by Gille & Goody (1964). Long, extremely fine wires of copper and constantan were connected to the floating member to make the temperature measurements possible. These fine wires did produce a torque on the system, but this was sufficiently constant during a run so that an accurate determination of the momentum flux was possible.

3.2. *Physical specifications*

The apparatus was entirely supported by a central shaft, specially turned from hardened stainless steel (figure 1). The shaft and housing (also of hardened stainless steel) formed the mating units of the air bearing, which supported the lower half of the convection apparatus. An adjustable thrust bearing, consisting of a micrometer head rigidly attached to a bronze sleeve, supported the upper half of the convection apparatus. Thus the upper and lower assemblies were free to rotate independently about the central axis.

The air bearing was a modification of a design described by Adams (1958). With a filtered supply of air at 20 p.s.i., the air bearing provided a rigid support eliminating all modes of motion except rotation about a vertical axis. The constant flow of air (about $\frac{1}{2}$ cu.ft./min) introduced small turbine torques, but these remained constant provided the lower member was allowed to rotate through only a small arc.

Each half of the apparatus consisted of an aluminium disk, 24 in. in diameter and $\frac{2}{3}$ in. thick. On the inner surface of each disk a formica sheet, $\frac{1}{8}$ in. thick,

was bonded. To these were bonded aluminium plates, $\frac{3}{16}$ in. thick, which made contact with the fluid. These were carefully turned to be flat and parallel; variations in the plate spacing were about ± 0.0007 in. at the rim, or about 1 % of the smallest spacings studied. In these experiments the greatest plate separation was 1 in. approximately.
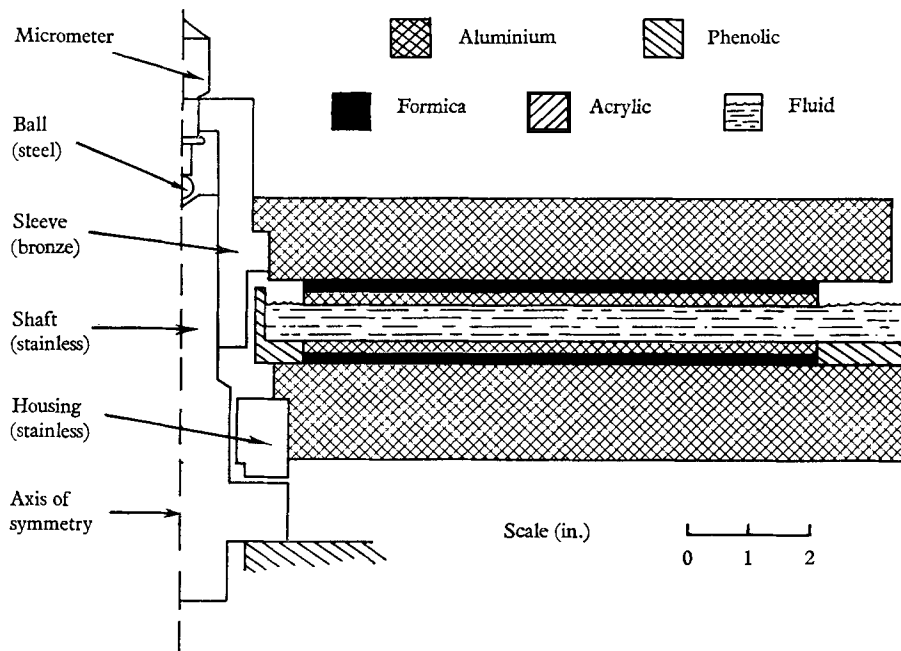

FIGURE 1. Cross-section of the apparatus in a vertical plane
through the axis of symmetry.

The fluid was contained laterally by walls at radii $r = 1.5$ in. and $r = 12$ in. The test section, the region between the aluminium plates, extended from $r = 2$ in. to $r = 10.5$ in. The extended edge regions were important in order that the effect of the rigid side walls on the velocity distribution in the test section be slight. Heat loss and fluid loss by evaporation were limited by leaving only $\frac{1}{16}$ in. clearance between the ring at $r = 12$ in. and the circumference of the upper disk.

In the experiment, three fluids were used: two light grades of Dow Corning 200 fluid, a clear Silicone oil, and a highly refined kerosine. We found the Prandtl numbers of these fluids to be 9·35, 21·72 and 29·93, respectively. We were limited to this range by several factors. In the first place, there are no liquids with Prandtl numbers significantly below 9·35 at room temperature, except for mercury, which would require a redesign of the experiment. Secondly, we could not use fluids of higher Prandtl number and still obtain values of Mo significantly greater than unity.

Heating was supplied by a 300 W coil attached to the underside of the lower disk (not shown in figure 1). This was backed by 2 in. foam rubber to decrease heat loss. The outer surface of the acrylic ring and the top surface of the upper

disk were also encased in thermal insulation. Cooling was achieved by allowing ice to melt on the top surface of the upper disk. The average temperature of the system was always within $\pm 1\,^\circ$C of room temperature, which was controlled to $\pm \frac{1}{2}\,^\circ$C. Temperature differences across the plates ranged from about $7\,^\circ$C at the start of a run to $0\cdot 7\,^\circ$C at the end. A typical run took 2–3 h.

The rotation of the upper disk was supplied by a variable speed Graham transmission, reduced 300:1 in two stages. An ordinary V-belt provided the linkage to a large pulley attached to the upper disk. A typical angular velocity was $0\cdot 01$ rad/ sec. Variations in the rotation rate were measured, but these produced torque changes well below the noise level of our measurements.

3.3. *The torque measurements*

Torque measurements were made with the lower member stationary. A balance of torques was obtained by twisting a quartz fibre which was attached to the floating member by means of a rigid U-shaped frame (figure 2). With an optical
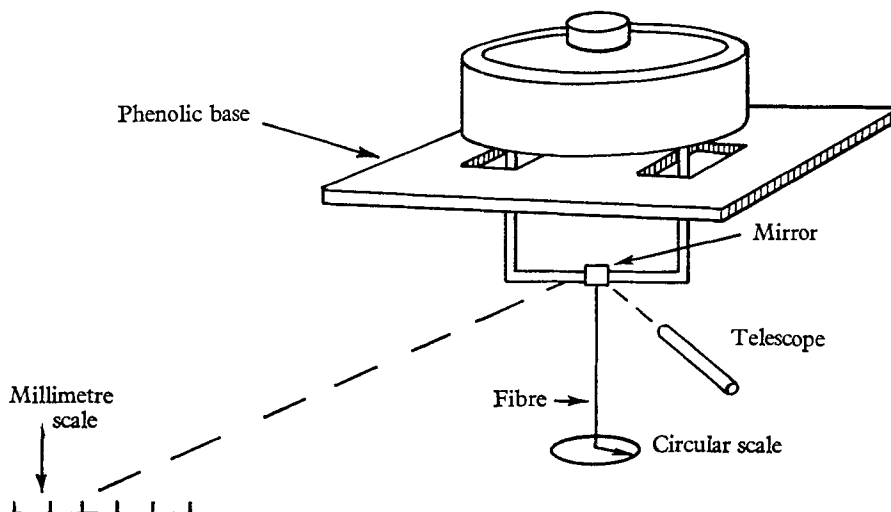

FIGURE 2. The system for measuring torque.

lever, angular accelerations as small as 10^{-7} rad/sec^2 were detectable. Before and after a run, the balance position of the fibre was noted with both plates stationary. The difference between this null value and the fibre position during a run was then a measure of the fluid mechanical torque.

The sensitivity of the system was about $\frac{1}{2}$ dyne cm of torque, although noise levels were several times higher due to slow drift of the null position. The major sources of this drift were currents in the surrounding air. The whole apparatus was enclosed in a cardboard box, which eliminated the gross 'wind', but air motions within the box due to changes in room temperature caused observable fluctuations in the torque on the system. It was also necessary to balance and level the lower member to avoid gravitational torques. Finally, care was taken to minimize torques due to the fine (38-gauge) thermocouple wires.

The experimental apparatus, used as a viscometer, provided a means of calibrating the fibre. A stable density gradient was imposed, and the fibre twist was noted at several rotation speeds and plate separations, for three fluids of known viscosity. In calculating the expected torque, account was also taken of the fluid in the edge regions, and of the air in the narrow gap between the upper and lower assemblies (figure 1). Fortunately, these additional torques remain roughly constant as the plate spacing d is decreased, whereas the torque transmitted by the fluid in the test section becomes infinite as d^{-1}. Thus by properly varying the spacing, and by using different fluids, one is able to separate the various torques, and to obtain estimates of each.

In practice, the edge-region torque was estimated theoretically, assuming molecular diffusion of momentum in the edge region. The air-friction torque and the fibre calibration were then obtained simultaneously using the method of least squares (Whittaker & Robinson 1930). In minimizing the mean squared deviation, equal weight was given to equal errors in the torque measurement. In this way we were able to obtain the fibre calibration to ± 4%, and the air friction correction to ± 22%, standard deviation. The r.m.s. error was about 3 dyne cm, which is in accord with observed fluctuations in the null position of the fibre.

Having calibrated the fibre, we may then obtain *Mo* for runs with convection, defined as the torque due to the fluid in the test section, divided by the conductive torque. Corrections were also made for the edge regions, and for air friction as described above. The edge-region torque was assumed to be a constant fraction of the total torque at all Rayleigh numbers. The fraction (8%) was an estimate based on applying mixing-length theory to the edge region, assuming the same boundary-layer structure as in the test region. The air-friction correction was always less than 6% of the total torque. The fractional error in the determination of *Mo* depended, of course, on the magnitude of the measured torque, and therefore on the angular velocity of the upper plate.

3.4. *The temperature measurements*

Let us define T_1 and T_4 as the temperatures of the upper and lower aluminium disks, respectively. Let the temperatures of the upper and lower aluminium plates, which are in contact with the fluid, be T_2 and T_3. Then, in order to measure the heat flux and the Rayleigh number, it is necessary to know the quantities

$$\left. \begin{aligned} \Delta T_R &= T_3 - T_2, \\ \Delta T_H &= (T_4 - T_1) - (T_3 - T_2). \end{aligned} \right\} \tag{20}$$

The Rayleigh number is given by (7), with ΔT replaced by ΔT_R. In a steady state, the heat flux will be $k_I \Delta T_H / (2d_I)$, where k_I and d_I are the thermal conductivity and thickness of the insulating formica sheets.

For the thermally decaying system, we may obtain a more accurate expression for the heat flux by expanding in the time derivative. Then the heat flux at the boundary of the plate and the fluid is given by

$$\frac{k_I}{2d_I} \Delta T'_H \equiv \frac{k_I}{2d_I} \left[\Delta T_H - (s_A + \tfrac{1}{2} s_I) \frac{d\Delta T_R}{dt} - (\tfrac{1}{6} s_I) \frac{d\Delta T_H}{dt} \right], \tag{21}$$

where $s_A = \rho_A c_A d_A d_I / k_I$ and $s_I = \rho_I c_I d_I^2 / k_I$. The subscript A stands for the aluminium plates and the subscript I for the insulating formica sheets. Here ρ, c, d and k are the density, specific heat, thickness and thermal conductivity of the material, respectively. Equation (21) corrects an expression obtained by Malkus (1954a). For our experiment, the correction terms in (21) were about 5 % of the total heat flux.

Copper–constantan thermocouples were used to measure these temperatures. In bonding the formica sandwiches, the thermocouples were placed in contact with the aluminium on either side of the formica. The wires from the rotating member were connected to the recording equipment through mercury contacts. Wires from the floating member were connected to long, fine wires in order to minimize torque. Rectified radio pick-up in these large circuits was the principal source of error in the temperature measurements, and amounted to 0·03 °C at times. In addition, systematic errors occurred at the start of a run, before the system had settled down to the quasi-steady decay assumed in the derivation of (21). Other sources of error include the mercury contacts, variations among the thermocouples, and the non-linearity of the e.m.f.-temperature curve. These caused errors of less than 0·01 °C in the temperature measurements, however.

The Nusselt number is given by the quantity $\Delta T_H'$ in (21), divided by its value for the conductive state. In order to obtain a conductive state, a stable stratification was imposed, and measurements were made at different plate separations, as in the preceding section. Again, correction was made for the heat transport in the edge region, and for heat leakage in the solid boundaries. These corrections were always less than 4 % of the total heat transport. Using the method of least squares, the conductive value of $\Delta T_H' d / \Delta T_R$ for each fluid was obtained to $\pm 1\cdot5$ %, standard deviation, where d is the depth of the fluid. These values were obtained under the optimum experimental conditions, however. At the beginning and end of a run, the uncertainty in measurements of the Rayleigh number and the Nusselt number was perhaps ± 5 %, due to the systematic errors mentioned above. These errors fluctuated quite slowly, and therefore introduced a small systematic bias into the data of a single run. We shall refer again to this problem in discussing the experimental results.

3·5. *Physical constants of the fluid*

In order to specify the Reynolds number at any point in the fluid, it was necessary to know the viscosity, ν. This was measured with a Cannon Fenske Viscometer (A.S.T.M. Standards, Designation D 445), calibrated with distilled water. For the three fluids studied we found $\nu = 0\cdot00675$, $0\cdot0160$ and $0\cdot0236$ cm²/sec. The uncertainty of the measurement was about $\pm 1\cdot5$ %.

The Prandtl number is the ratio ν/κ, where $\kappa = k/(\rho c)$, and k is the thermal conductivity, ρ the density and c the specific heat of the fluid. We measured c by heating a known mass of the fluid in a Dewar flask, as described by Rice (1949). Water was used to calibrate, and we may place the error of the measurement at ± 2 %. The thermal conductivity k is directly related to the quantity $\Delta T_H' d / \Delta T_R$ for the conductive state, discussed in the last section. Again, water

was used to calibrate the apparatus. From this, we may specify k to $\pm 3\%$, and so the uncertainty in σ was about $\pm 4\%$, standard deviation.

The Rayleigh number R depends on the depth d, the temperature ΔT_R, and the quantity $\alpha g/(\kappa \nu)$. This last quantity was measured directly by observing Nu vs. R for $R \approx 1708$ and both plates stationary. We located the sharp transition below which $Nu = 1$, and assumed that $R = 1708$ at that point. $R_0 = 1708$ is the theoretical value of the Rayleigh number below which steady convection is impossible. This was obtained by Pellew & Southwell (1940), and verified experimentally by many people, *e.g.* Silveston (1958). We were thus able to measure $\alpha g/(\kappa \nu)$ to $\pm 3\%$, assuming that the theoretical value applies to this experiment.

4. Experimental results

4.1. *Comparison with the mathematical model*

The mathematical model defined at the outset of this paper only approximately describes the physical system encountered in the experiment. The Boussinesq equations neglect accoustical effects, dissipative heating and compressibility. For thermal convection in the laboratory, these are good approximations. However, it is not clear that we may also neglect the temperature variation of α, ν and κ. In particular for kerosine, ν varies by about 15% in a temperature range of $7\ ^\circ\mathrm{C}$, which is about the maximum range in these experiments. However, because of the symmetry of the Boussinesq equations between top and bottom, Nu and Mo will only be affected to second order in the magnitude of this variation.

We have also assumed that the relative motion of the plates was rectilinear, and that the lateral boundaries were infinitely far away. Thus the scale of the motion must be small compared to lateral scales. If we accept the mixing-length analysis, this means that z_ν must be small. Using equation (13), this internal scale was always less than $\frac{1}{10}$ the inner radius of the annular basin, and $\frac{1}{50}$ the outer radius. Thus it seems valid to neglect the side boundaries and the curvature of the mean flow.

We have also neglected the change in the Rayleigh number with time due to the decay nature of the experiment. In order that the instantaneous fluxes be close to the steady-state values, the adjustment rate of the convection must be rapid compared to the decay rate of the Rayleigh number. The latter quantity, $-\dot{R}/R$, is equal to about $0.3 \times 10^{-3}\,\mathrm{sec}^{-1}$ in this experiment. The adjustment rates κ/z_κ^2 and ν/z_ν^2 are over 100 times larger, and thus we may expect only a slight lag in the structure of the flow.

The centrifugal acceleration of the fluid at the rotating upper plate was also neglected. However, the secondary circulation due to this acceleration will cause additional fluxes of heat and momentum. These will depend strongly on the rotation rate Ω, whereas the quantities Nu and Mo were assumed independent of Ω. In the experiment, Mo was measured in the range

$$0.0015 < \Omega < 0.05\,\mathrm{rad/sec}.$$

Nu was measured in this range, and also for $\Omega = 0$. We found that Mo and Nu

vary less than 5 % for $\Omega < 0.015$ rad/sec, and therefore our analysis of the data was limited to this range. At higher rotation rates Nu decreases and Mo increases.

Besides the secondary circulation, the mean shear itself may cause a dependence of Mo and Nu on Ω, for Ω large enough. In our mixing-length theory, however, we assumed that the mean shear was a passive quantity. Thus by empirically limiting our data to $\Omega < 0.015$ rad/sec, we are also assuring that the non-linear effects of the shear be small.

4.2. *Heat transfer*

Equation (18) gives a prediction from mixing-length theory of the dimensionless heat flux at large Rayleigh numbers and large Prandtl numbers. This relation has the form

$$Nu = c_1 R^{\frac{1}{3}}, \quad c_1 \sim 0.089. \tag{22}$$

Originally, (22) was derived for no mean shear, $Re = 0$. We have argued that it should continue to hold for small rates of shear, and will now describe an empirical test of this assumption.

In figure 3 we have plotted Nu vs. $(R/R_0)^{\frac{1}{3}}$, where $R_0 = 1708$ is the critical Rayleigh number. The data are for a single fluid ($\sigma = 29.93$); the points A, B, C are runs with no rotation ($\Omega = 0$), and the points D, E, F are runs for which $\Omega = 0.015$ rad/sec. Each run covers approximately the same temperature range; the temperature difference between the plates is 6–7 °C at the beginning of a run, and 0.7–0.8 °C at the end. However, the plate separation for A, B, C, was roughly 1 in., $\frac{1}{2}$ in., $\frac{1}{4}$ in., respectively, and similarly for D, E, F. Therefore the runs cover different ranges of R and Nu, as shown in the graph. The fact that these different runs join is partial confirmation of the validity of our experimental method. For some of the data, discrepancies of several percent occurred due to systematic errors in the temperature measurements.

The effect of rotation on Nu is clearly discernible in the graph but it is not more than 5–6 %. For smaller rotation rates, and for fluids with smaller Prandtl numbers ($\sigma = 9.35$ and 21.72), the effect is still smaller. The relation between Nu and $R^{\frac{1}{3}}$ appears to be linear over the range shown in the graph ($Nu \leqslant 15$). For the other fluids, it was possible to achieve somewhat larger values of R and Nu; for $\sigma = 9.35$, the linear relationship appears to hold for $Nu \leqslant 25$. In figure 4, we have plotted Nu vs. $(R/R_0)^{\frac{1}{3}}$ for all three fluids, with both plates stationary. Certainly the dependence of Nu on σ is not great, for $\sigma = 9.35$, 21.72 and 29.93. This agrees qualitatively with the behaviour in (22), as obtained from mixing-length theory.

We have also analyzed the heat-transport data numerically, for both plates stationary. Using the method of least squares, we fitted the data for each fluid and $R/R_0 \geqslant 5$ to a curve of the form

$$Nu = c_1(R)^{\beta} + c_2. \tag{23}$$

We gave equal weight to equal values of ΔT_H, which is the measured quantity most closely related to the heat flux, as given in equation (21). One finds that

the departures from (23) are statistically significant at the 1% level except when

$$0\cdot30 \leqslant \beta \leqslant 0\cdot32 \quad (\sigma = 9\cdot35),$$
$$0\cdot25 \leqslant \beta \leqslant 0\cdot33 \quad (\sigma = 21\cdot72),$$
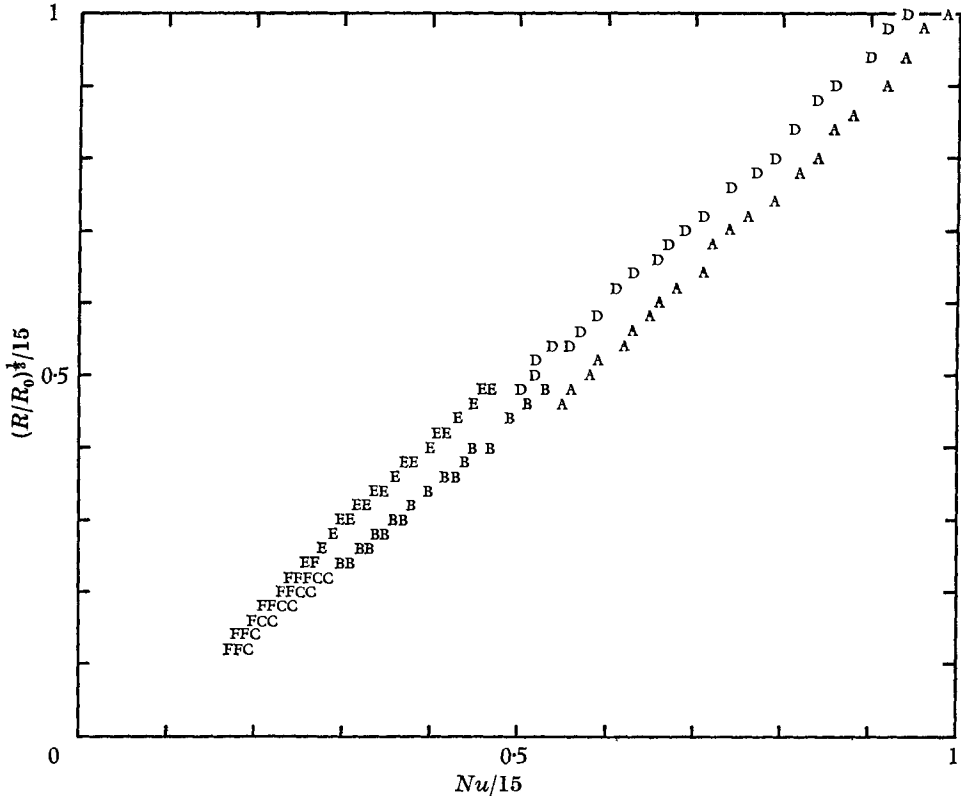$$0\cdot29 \leqslant \beta \leqslant 0\cdot32 \quad (\sigma = 29\cdot93).$$
$$\tag{24}$$

FIGURE 3. Experimental plot of $(R/R_0)^{\frac{1}{3}}/15$ vs. $Nu/15$, with $\sigma = 29\cdot93$ and $\Omega = 0$ (A, B, C) and $\Omega = 0\cdot015$ rad/sec (D, E, F). This and the following three graphs were drawn by computer. The scaled variables are plotted in the range (0, 1); the abscissa is given to the nearest $0\cdot01$ and the ordinate to the nearest $0\cdot02$. Data from a single experimental run are represented by the same letter of the alphabet. When points coincide, only the letter highest in the alphabet is printed.

Thus the departures of the data from the $R^{\frac{1}{3}}$ law in (22) are statistically significant. However, these data are based on a limited number of experimental runs (for $Re = 0$), and so the errors in the temperature measurements may have influenced the result (24) in a systematic way. Therefore one should not consider these departures to be physically significant.

Then, if we choose $\beta = \frac{1}{3}$ in (23), we obtain

$$c_1 = 0\cdot0784, \quad c_2 = 0\cdot77 \quad (\sigma = 9\cdot35, \quad \zeta \leqslant 15 \times 10^3),$$
$$c_1 = 0\cdot0820, \quad c_2 = 0\cdot86 \quad (\sigma = 21\cdot72, \quad \zeta \leqslant 5 \times 10^3),$$
$$c_1 = 0\cdot0827, \quad c_2 = 0\cdot82 \quad (\sigma = 29\cdot93, \quad \zeta \leqslant 4 \times 10^3),$$
$$\tag{25}$$

where $\zeta = R/R_0 = R/(1708) \geqslant 5$. The values of c_1 in (25) are in quite good agreement with Kraichnan's theoretical estimate $c_1 \sim 0.089$ in (22). These results are also consistent, over this particular range of σ, with other experimental data. Malkus (1954a) describes his data in the form (22) with $c_1 = 0.0794$. Globe & Dopkin (1959) give

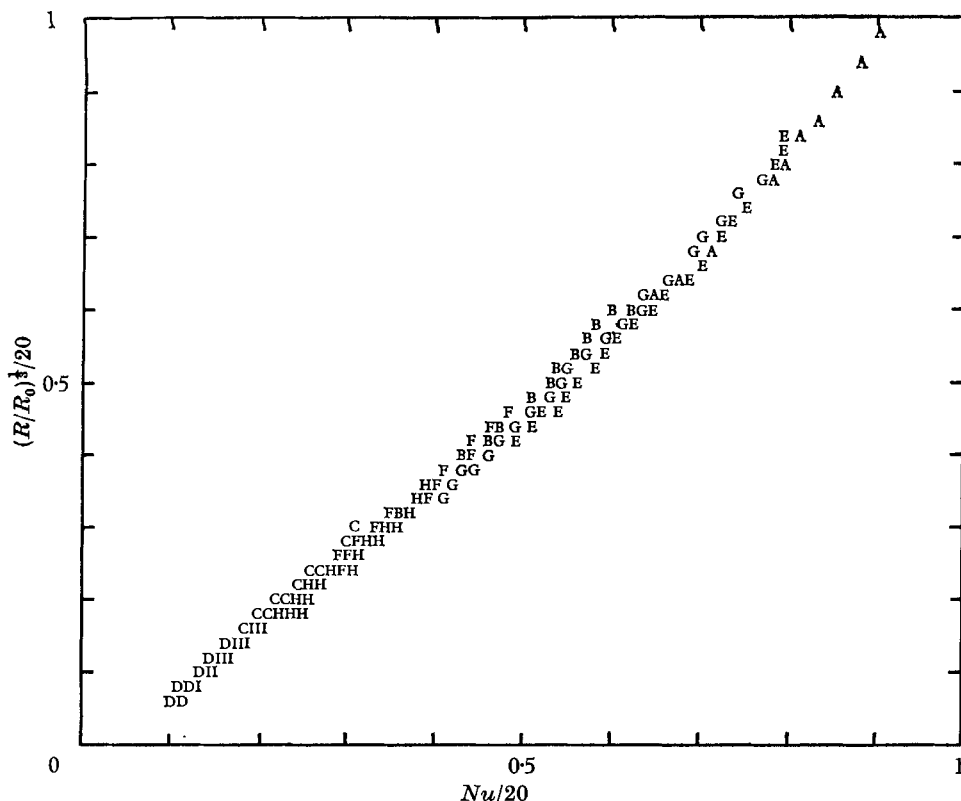$$Nu = 0.069\,(R)^{\frac{1}{3}}\,(\sigma)^{0.074}, \tag{26}$$

FIGURE 4. Experimental plot of $(R/R_0)^{\frac{1}{3}}/20$ vs. $Nu/20$, with $\Omega = 0$ and $\sigma = 9.35$ (A, B, C), $\sigma = 21.72$ (D, E, F) and $\sigma = 29.93$ (G, H, I). See figure 3 for further explanation.

for which $c_1 = 0.0814$, 0.0864 and 0.0887, for $\sigma = 9.35$, 21.72 and 29.93, respectively. Silveston (1958) gives

$$Nu = 0.10(R)^{0.31}\,(\sigma)^{0.05}, \tag{27}$$

which yields comparable values of Nu for σ in the range 10–30 and $\zeta \sim 10^2 - 10^3$.

Thus our measurements of Nu are in satisfactory agreement with mixing-length theory, and with previous experiments. We have located a value of Ω below which the dependence of Nu on Re is small, and we have restricted our analysis to this range.

4.3. *Momentum transfer*

Mixing-length theory predicts (19), for R and σ large. This may be written

$$Mo = B_1 Nu\sigma^{-\frac{1}{2}} \quad (B_1 \sim 0\cdot316). \tag{28}$$

Again, this relation should hold only in the limit as $Re \to 0$, for which the shear is a passive quantity. In figure 5 we have plotted $Mo - 1$ vs. Nu for $\sigma = 21\cdot72$ and $0\cdot007 \leqslant \Omega \leqslant 0\cdot015$ rad/sec. Although the angular velocity Ω varies by a
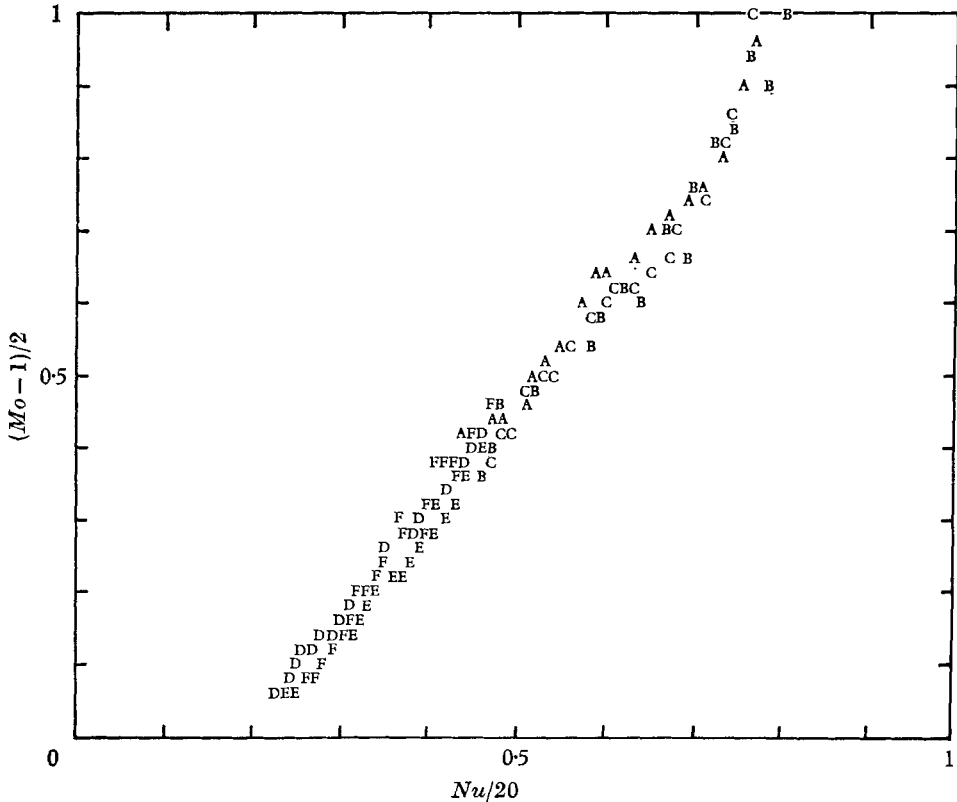

FIGURE 5. Experimental plot of $(Mo-1)/2$ vs. $Nu/20$, with $\Omega \leqslant 0\cdot015$ rad/sec and $\sigma = 21\cdot72$. See figure 3 for further explanation.

factor of two, Mo does not seem to be a function of Ω, for the data shown in the graph. Thus the dependence of Mo on Re appears even less pronounced than the dependence of Nu on Re, for the same range of Re. This is somewhat misleading, however, since the scatter of the experimental data is greater in figure 5 than in figure 3. However, in no case was the change of Nu or Mo greater than 5 % in the range $0 \leqslant \Omega \leqslant 0\cdot015$ rad/sec, and so we have restricted our discussion to this range.

We also note the good agreement between runs A, B, C, for which the depth was 1 in., and the runs D, E, F, for which the depth was $\frac{1}{2}$ in. This is another confirmation of the validity of our experiment. Further, we note that Mo and Nu appear to be linearly related for Mo greater than about $1\cdot1$. This is especially striking since the measurements cover the range $Mo \leqslant 3$, whereas mixing-length

theory applies only for Mo large. (For $\sigma = 9\cdot35$, it was feasible to measure to $Mo \leqslant 5$; for $\sigma = 29\cdot93$, only $Mo \leqslant 2\cdot5$ was feasible.) The range of Mo studied is perhaps an important limitation of this experiment. Nevertheless, one may obtain the slope in figure 5 with considerable accuracy, and then interpret the data assuming this linear relation to hold to very high values of Mo. This is the point of view taken in the interpretation which follows.
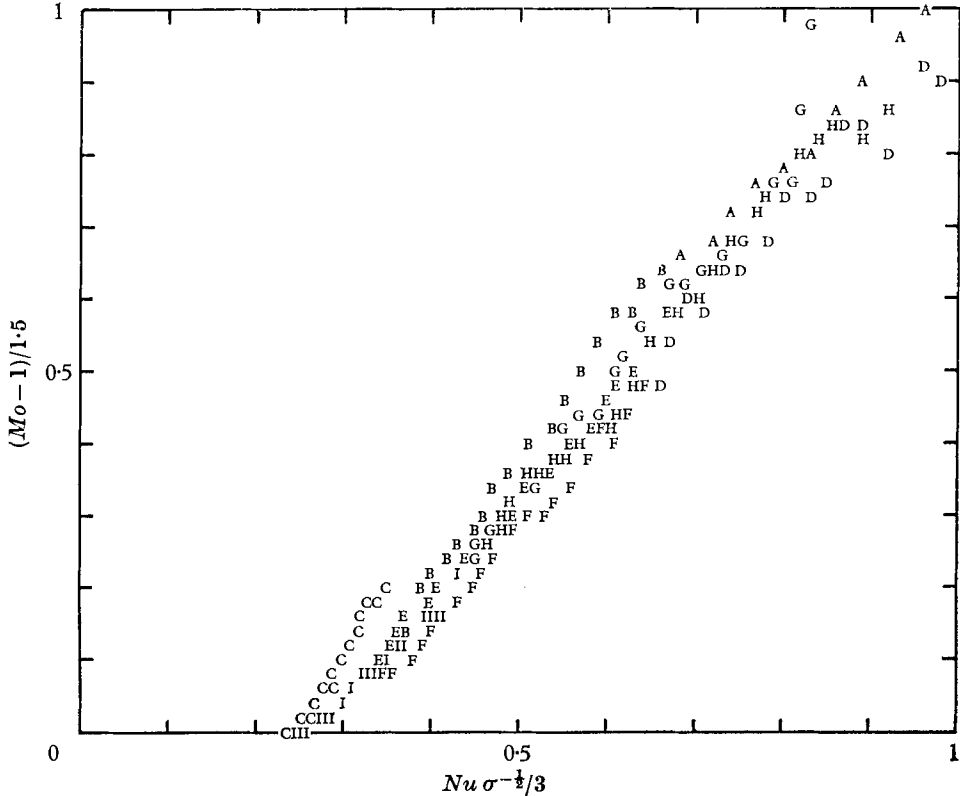

FIGURE 6. Experimental plot of $(Mo-1)/1\cdot5$ *vs.* $Nu\sigma^{-\frac{1}{2}}/3$, with $\Omega \leqslant 0\cdot015$ rad/sec and $\sigma = 9\cdot35$ (A, B, C), $\sigma = 21\cdot72$ (D, E, F) and $\sigma = 29\cdot93$ (G, H, I). See figure 3 for further explanation.

If we graph $Mo-1$ *vs.* $Nu\sigma^{-\frac{1}{2}}$, as in figure 6, we find that the data from all three fluids lie approximately on the same straight line. On the other hand, if $Mo-1$ is plotted against Nu, or against $Nu\sigma^{-1}$, the data for the three fluids are distinct. This implies that (28) does in fact describe the data; from numerical analysis we may formulate this conclusion more exactly.

As before, the data for each fluid were fitted to a curve of the form

$$Mo = b_1(Nu)^\beta + b_2, \tag{29}$$

by minimizing the weighted sum of squared deviations from this curve. The weighting was chosen so that equal errors of torque were given equal weight. In this way, the runs at slower rotations, where the error in Mo is large, were given proportionately less weight than the runs at faster rotations. We also

15

took into account errors in the null position of the fibre, which was measured before and after each run. In calculating the uncertainty of the regression coefficients we again followed Whittaker & Robinson (1930). About 30 runs were analyzed.

Our first aim was to test the linearity of the relationship between Mo and Nu. The data were inconsistent with (29) except for

$$\left.\begin{aligned}
0{\cdot}90 \leqslant \beta \leqslant 1{\cdot}20 \quad (\sigma = 9{\cdot}35), \\
0{\cdot}90 \leqslant \beta \leqslant 1{\cdot}15 \quad (\sigma = 21{\cdot}72), \\
0{\cdot}80 \leqslant \beta \leqslant 1{\cdot}35 \quad (\sigma = 29{\cdot}93).
\end{aligned}\right\} \tag{30}$$

Thus the experiment is consistent with the assumption $\beta = 1$ in (29). We may therefore assume $\beta = 1$ in order to compare the coefficients b_1 and b_2 with theoretical predictions. The results of numerical analysis are given in table 1.

σ	b_1	b_2
9·35	0·227 ± 0·005	0·518 ± 0·026
21·72	0·160 ± 0·007	0·360 ± 0·059
29·93	0·127 ± 0·005	0·442 ± 0·040

TABLE 1. The empirical coefficients b_1 and b_2 in the equation
$$Mo = b_1 Nu + b_2$$

We also wish to obtain the Prandtl-number dependence of b_1 and b_2, assuming a power-law relationship of the form

$$b_1 \propto \sigma^{-n}; \quad b_2 \propto \sigma^{-m}. \tag{31}$$

From the data we may determine the ranges of n and m over which (31) does not hold, *e.g.* for which the quantities $\sigma^n b_1$, and $\sigma^m b_2$, will depend linearly on σ. Using the error estimates in table 1, we find the data to be inconsistent with (31) except when

$$0{\cdot}40 \leqslant n \leqslant 0{\cdot}60, \qquad -0{\cdot}05 \leqslant m \leqslant 0{\cdot}40. \tag{32}$$

The values $n = 0{\cdot}50$ and $m = 0{\cdot}0$ are not excluded at the 5 % level. For these values, the best fit to all the data is the line

$$Mo = (0{\cdot}71) Nu \sigma^{-\frac{1}{2}} + (0{\cdot}44). \tag{33}$$

The statistical result (32) provides good evidence that $Mo \sim Nu\sigma^{-\frac{1}{2}}$, at large Rayleigh numbers. This is the type of behaviour predicted from mixing-length theory, equation (28), although the numerical constant B_1 in (28) appears to be too small by a factor greater than 2. In view of the difficulty of estimating these numerical constants theoretically, we do not regard this discrepancy as a serious one.

5. Conclusion

We have shown the usefulness of mixing-length theory in predicting the mean fluxes of heat and horizontal momentum in this experiment. For small rates of shear, we find that the momentum flux is proportional to the imposed velocity

difference, and that the heat flux is independent of this difference. These statements are embodied in equations (8) and (9), which we have verified experimentally. Further, we have demonstrated that the mean fluxes are independent of the plate separation d, for d large, as implied by (10) and (11). This requires a boundary-layer structure which is independent of the large-scale turbulent flow in the interior. Finally, we have demonstrated that Kraichnan's mixing-length theory accurately describes the dependence of this boundary-layer structure on the molecular diffusivities ν and κ.

The importance of this result is that one may apply mixing-length theory to other turbulent flows. For instance, we may speculate on the effects of a finite shear in the present experiment. As the shear is increased, the length $z_s = \nu M^{-\frac{1}{2}}$ decreases. When $z_s \sim z_\nu$, the eddy viscosity at $z = z_\nu$ will be enhanced due to turbulence generated by the mean shear. Thus the momentum transport and *Mo* will increase. On the other hand, this shear turbulence will be small at the inner boundary layer $z = z_\kappa$. At that level, vertical velocities due to the shear will be much less important than the mean shear velocity itself. This adds a term $\bar{u} w_x$ on the left of (14). Roughly speaking, the effect of this term is to generate a component of w which is $\frac{1}{2}\pi$ out of phase with θ. Therefore, this component is an energy sink, and serves to decrease the energy available for the component in phase with θ, and therefore to decrease the heat transport. Alternately, one may imagine the mean shear pulling the convective elements apart at $z = z_\kappa$, thereby making them less able to convect heat against dissipation.

In fact, as the shear was increased in this experiment, *Mo* increased and *Nu* decreased, in accord with these predictions. We have experimental evidence that this effect was due to shear itself, and not to rotational effects. That is, comparing this data with data obtained on a smaller preliminary apparatus, we find the non-linear effects of shear to depend on the Reynolds number at the rim, $r\Omega d/\nu$, rather than the Taylor number, $\Omega d^2/\nu$.

Mixing-length theory has been used to predict the mean profiles of temperature and velocity in the atmospheric boundary layer (*e.g.* Priestley 1959). In comparing the present experiment with atmospheric data, it is useful to estimate the Richardson number,

$$Ri = \alpha g \frac{d\bar{T}}{dz} \Big/ \left(\frac{d\bar{u}}{dz}\right)^2,$$

for the flow in this experiment. According to mixing-length theory as presented here, the minimum value of $-Ri$ occurs at the height $z = z_\nu$; this is

$$Ri = -\frac{30}{4} \frac{R\,Nu}{(\sigma Re\,Mo)^2}.$$

Then if *Re* is the Reynolds number at the rim, we find that non-linear effects of shear become important at $-Ri = 10$, approximately, and thus our data analysis was restricted to more negative values of *Ri*. In the atmosphere, however values of *Ri* below -1 or -2 are rarely observed in steady conditions, and so we have not modelled the atmosphere in detail, even in the turbulent interior region. On the other hand, we have demonstrated the usefulness of similarity

theory in problems of convection with shear, and we suggest that one might predict heat and momentum fluxes in the atmosphere using this type of approach.

REFERENCES

ADAMS, C. R. 1958 *Product Engineering,* **29** (50), 96.

A.S.T.M. Standards 1964 Pt. 17, 164.

BATCHELOR, G. K. 1953 *The Theory of Homogeneous Turbulence.* Cambridge University Press.

CHANDRASEKHAR, S. 1961 *Hydrodynamic and Hydromagnetic Stability.* Oxford University Press.

GILLE, J. & GOODY, R. 1964 *J. Fluid Mech.* **20,** 47.

GLOBE, S. & DROPKIN, D. 1959 *Trans. A.S.M.E. J. Heat Transfer,* **81,** 24.

HERRING, J. R. 1964 *J. Atm. Sci.* **21,** 277.

KRAICHNAN, R. H. 1962 *Phys. Fluids,* **5,** 1374.

MALKUS, W. V. R. 1954*a* *Proc. Roy. Soc.* A, **225,** 185.

MALKUS, W. V. R. 1954*b* *Proc. Roy. Soc.* A, **225,** 196.

MALKUS, W. V. R. 1956 *J. Fluid Mech.* **1,** 521.

MALKUS, W. V. R. 1960 *Theory and Fundamental Research in Heat Transfer,* p. 203. (Ed. J. A. Clark). Oxford: Pergamon Press.

MONIN, A. S. & OBUKHOV, A. M. 1953 *Doklady Akad. Nauk S.S.S.R.* **93,** 257.

PELLEW, A. & SOUTHWELL, R. V. 1940 *Proc. Roy. Soc.* A, **176,** 312.

PRIESTLEY, C. H. B. 1959 *Turbulent Transfer in the Lower Atmosphere.* University of Chicago Press.

RICE, R. B. 1949 *A.S.T.M. Bulletin,* no. 157. (March 1949), 72.

SILVESTON, P. L. 1958 *Forsch. Gebiete Ingenieurwes,* **24,** 29, 59.

WHITTAKER, E. T. & ROBINSON, G. 1930 *The Calculus of Observations,* 2nd edn. Princeton, N.J.: D. Van Nostrand Co., Inc.